EPSC Abstracts
Vol. 10, EPSC2015-610, 2015
European Planetary Science Congress 2015

Impact of Radiatively Active Water Ice Clouds in the GEM-Mars GCM

L. Neary and F. Daerden
Belgian Institute for Space Aeronomy, Brussels, Belgium (lori.neary@aeronomie.be)

Abstract

Water ice clouds have proven to be an important driver in the temperature distribution and overall climate of the Martian atmosphere. Clouds have both a direct and indirect radiative effect on temperature and circulation, which in turn can modify the water vapour distribution and that of other trace gases.

We have included the radiative effect of water ice clouds (RAC) in the GEM-Mars GCM model, using Mie code and optical indices to compute the scattering properties of ice particles.

We present preliminary results from simulations with and without RAC, and compare these initial tests with Mars Climate Sounder (MCS), Thermal Emission Spectrometer (TES) and Mars Color Imager (MARCI).

The GEM-Mars model

GEM-Mars is a three-dimensional general circulation model (GCM) of the Mars atmosphere extending from the surface to approximately 150 km based on the GEM (Global Environmental Multiscale) model, the operational data assimilation and weather forecasting system for Canada (Côté et al., 1998). The dynamical core is an implicit two-time-level semi-Lagrangian scheme on an Arakawa C-grid with a log-hydrostatic-pressure terrain-following vertical coordinate discretized on a Charney-Phillips grid (Girard et al., 2014). The model has both a hydrostatic and non-hydrostatic formulation, providing a single platform for simulations on a variety of horizontal scales. The model code is fully parallelized using OMP and MPI.

The GCM includes the relevant physical processes such as CO_2 condensation, planetary boundary layer mixing, gravity wave drag and surface parameterisations. A simple water cycle, gas-phase chemistry and passive tracers are also included. Because of the vertical extent of the model, UV heating, non-LTE effects and molecular diffusion are also included.

The scattering and absorption effects of dust are taken into account and the model includes interactive dust lifting by saltation and dust devils, based on the work of Kahre et al. (2006) and Newman et al. (2002). Three particle sizes of dust are transported using the dynamical core and optical properties are those given by Wolff et al. (2006, 2009). The active dust scheme has been successfully utilized to examine dust layering as seen by the Phoenix lander (Daerden et al. 2015, submitted).

For water ice clouds, a uniform radius of 2 μm is used as a starting point, with optical properties calculated using the indices of Warren and Brandt (2008). A simple bulk condensation scheme is used at present. The modularity of the model permits the inclusion of a more sophisticated microphysical parameterisation such as that used by Daerden et al. (2010) at a later date.

Simulations performed

For these initial tests, the GEM-Mars model was run for one Martian year with and without the impact of radiatively active water ice clouds. Both runs kept the same settings for dust devil and wind lifting rates, and the opacities were not scaled to observed values (i.e. free-running advected dust tracers).

The horizontal resolution of the model is $4^\circ \times 4^\circ$ with 103 log-hydrostatic-pressure levels up to $\sim$150 km.

In the following sections, we discuss the impact of RAC on temperature, circulation, dust lifting, water vapour and ice, and ozone.

Temperature

Figure 1 shows the difference in zonal mean temperature profiles for 4 seasons for the simulations with and without RAC. There is a general equatorial warming around 10 Pa of 10-15° K, but greater for the L_s 90 season where clouds are more dominant. There is also

warming in the winter polar regions at the equinoxes. The RAC have a infrared cooling effect in the lower levels, which can be seen more clearly when the zonal means for day and night are separated (not shown here).

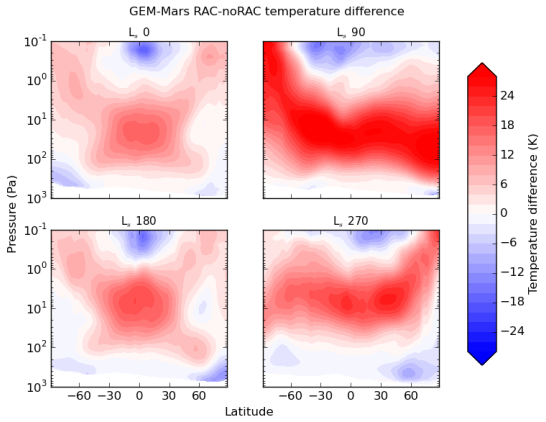

Figure 1: Temperature difference between the simulations with and without RAC. Red scale shows warming, blue shows a cooling effect.

We also compare the zonal mean temperature profiles with those from MCS (Kleinbohl et al., 2009) averaged over several years. Figure 2 shows the difference between the averaged MCS seasonal profiles and those of GEM-Mars. Before the introduction of RAC, the temperatures around 10 Pa region were too cold in the model (not shown), where now they are improved, with difference of less than 10 K depending on the season and location. The largest improvement was seen in the L_s 90 season, where water ice clouds form in the equatorial region. There are still some biases as the inclusion of RAC has indirect effects as well, such as influencing the amount of dust lifted off the surface and an increase in the strength of the Hadley cell circulation.

Impact on dust

An indirect effect of RAC is on the rate of dust lifting, which depends on the surface wind stress. A small decrease in wind stress due to RAC causes a decrease of nearly half in the optical depth due to lifted dust. The rate of dust lifted due to dust devils does not change as significantly. Figure 3 shows the zonal mean optical depth for the two simulations, separated into optical depth from dust devils and wind lifting.

Figure 4 shows the dust optical depth at the equator compared with TES (Smith et al., 2002). The dust in the model is not scaled to observations or tuned to any specific year, which can be done by adjusting an efficiency parameter or threshold. The timing of the dust storm compares well with TES in both cases but the values are too low, especially with the addition of RAC. Sensitivity tests are ongoing. Another factor in the dust optical depth is the change in circulation as discussed in the following section.

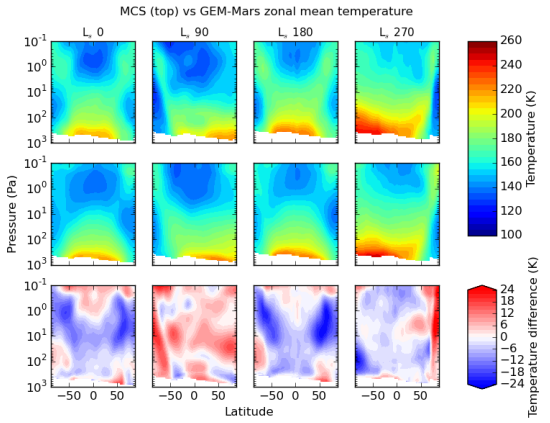

Figure 2: Averaged zonal mean temperature profiles from MCS (top), GEM-Mars with RAC (middle) and the difference (GEM-MCS) of the 2 fields (bottom). In the difference plots, blue indicates a cool bias in the model, red means the model is warmer than MCS.

Change in circulation

The inclusion of RAC increases the height of the Hadley circulation as suggested in Navarro et al. (2014). Figure 5 shows the change in zonal average mass stream function with the implementation of RAC. The circulation reaches higher in the atmosphere, which has a consequence of transporting the dust and water vapour to higher levels. For dust, there is a combination of reduced lifting as well as more transport, reducing the optical depth, although the reduced lifting is the dominant factor.

Impact on water vapour and ice

Due to the enhanced Hadley circulation, we see a decrease in the amount of total column water vapour, because it is transported higher in the atmosphere, reducing the column amount. The mean vertical profiles of ice extinction compare better with MCS with the inclusion of RAC (not shown here).

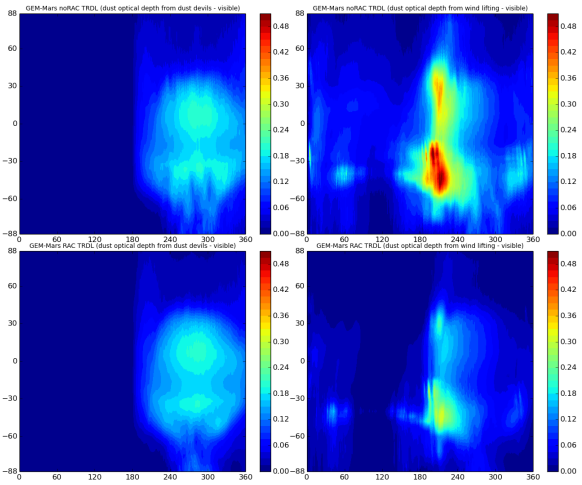

Figure 3: Dust optical depth for RAC and noRAC simulations. Top row is the RAC simulation, left: dust optical depth from dust devils, right: from wind lifting. Bottom row is the noRAC run, left: dust optical depth from dust devils, right: from wind lifting.

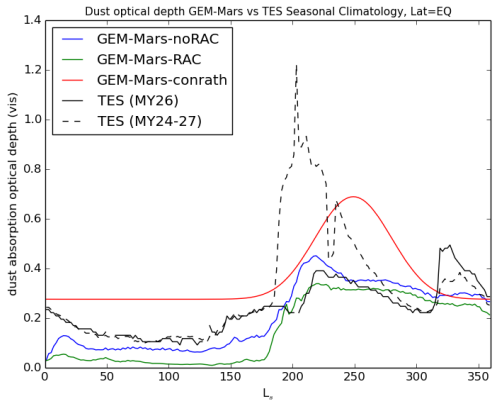

Figure 4: Dust optical depth compared with TES. The black solid line is TES, MY26 (a lower dust year) and the dashed line is the average from MY24-27. The RAC run is in green, without RAC is in blue and the climatological dust values previously used is given as a reference in red.

The complex interaction between dust, water vapour, ice and temperature make it difficult to quantify the direct effects of RAC. As these tests are preliminary, we have not tried to separate the direct and indirect effects and allowed the model to run without constraints. Sensitivity tests are necessary to understand more about these complexities.

The change in vertical distribution of water also impacts ozone as seen in the following section.

Ozone

Ozone reacts with the products of H_2O photolysis, leading to an anti-correlation between ozone and water vapour in the daytime. With the transport of water vapour to higher altitudes in the RAC simulation, we see a decrease in the the total column amount of ozone. Figure 6 shows a comparison of mean vertical profiles of ozone and water vapour for the two simulations. In the equinox seasons, especially in L_s 90, the layer of ozone at 10 Pa seen in the noRAC simulation is affected by the increased transport of water vapour in the RAC run.

Figure 7 shows this effect as compared with preliminary retrievals from the MARCI instrument (Malin et al., 2001). The inclusion of RAC reduces the column amount most significantly in the first half of the year, leading to better agreement with MARCI, notably at high latitudes in the northern summer, when the north polar permanent water ice cap is sublimating.

Summary and Conclusions

Overall, with the addition of RAC, temperatures in the 10 Pa region increased by 10-20 K, depending on season and location. The largest impact is during aphelion, where an equatorial cloud belt is formed. An indirect effect of RAC is on the amount of dust lifted which depends on the surface wind stress.

The increase in strength of the Hadley circulation has a significant impact on the vertical distribution of trace gases in the atmosphere.

It should be stressed that these are very initial tests, with no tuning of the dust or water cycle, but the results are very promising.

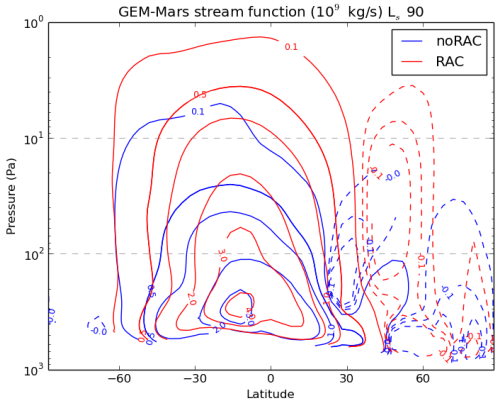

Figure 5: Zonal mean mass stream function in 10^9 kg/s for L_s 90, with (red contours) and without (blue) RAC. Positive solid lines indicate counter-clockwise flow.

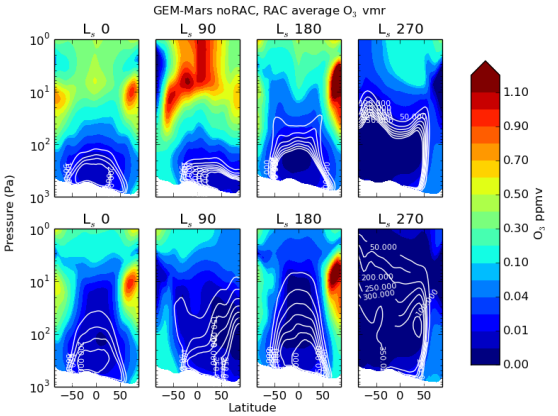

Figure 6: Top row is the noRAC simulation for 4 seasons and the bottom is with RAC. The colour contours are ozone mixing ratio and the white contours represent water vapour mixing ratios.

Acknowledgements

The research presented here has received support from the European Union Seventh Framework Program (FP7/2007-2013) under grant agreement no 607177, the CROSS DRIVE project. Thank you to R.T. Clancy for providing MARCI ozone data.

References

[1] Côté J., Gravel S., Méthot A., Patoine A., Roch M. and Staniforth, A., 1998. The operational CMC–MRB Global Environmental Multiscale (GEM) Model. Part I: Design considerations and formulation, *Mon. Wea. Rev.*, *126*(6), 1373–1395.

[2] Daerden, F., Whiteway, J.A., Davy, R., Verhoeven, C., Komguem, L., Dickinson, C., Taylor, P.A., Larsen, N., 2010. Simulating observed boundary layer clouds on Mars. *Geophys. Res. Let. 37*, L04203. doi:10.1029/2009GL041523

[3] Girard, C., Plante, A., Desgagné, M., McTaggart-Cowan, R., Côté, J., Charron, M., Gravel, S., Lee, V., Patoine, A., Qaddouri, A., Roch, M., Spacek, L., Tanguay, M., Vaillancourt, P.A., Zadra, A., 2014. Staggered Vertical Discretization of the Canadian Environmental Multiscale (GEM) Model Using a Coordinate of the Log-Hydrostatic-Pressure Type, *Mon. Wea. Rev.*, *142*, 1183–1196.

[4] Kahre M.A., Murphy, J.R., and Haberle, R.M., 2006. Modeling the Martian dust cycle and surface dust reservoirs with the NASA Ames general circulation model, *J. Geophys. Res.*, *111*, E06008.

[5] Kleinböhl, A., Schofield, J.T., Kass, D.M., Abdou, W.A., Backus, C.R., Sen, B., Shirley, J.H., Lawson, W.G., Richardson, M.I., Taylor, F.W., Teanby, N.A., McCleese, D.J., 2009. Mars Climate Sounder limb profile retrieval of atmospheric temperature, pressure, and dust and water ice opacity. *Journal of Geophysical Research* 114. doi:10.1029/2009JE003358

[6] Malin, M.C., Bell, J.F., Calvin, W., Clancy, R.T., Haberle, R.M., James, P.B., Lee, S.W., Thomas, P.C., and Caplinger, M.A., 2001. Mars Color Imager (MARCI) on the Mars Climate Orbiter. *J.Geophys. Res.*, *106*E8, 17651–17672.

[7] Newman C.E., Lewis, S.R., Read, P.L., Forget, F., 2002. Modeling the Martian dust cycle, 1. Representations of dust transport processes, *J. Geophys. Res.*, *107*(E12), 5123. doi:10.1029/2002JE001910

[8] Smith, M.D., Pearl, J. C., Conrath, B., Christensen, P.R., Thermal Emission Spectrometer results: Mars atmospheric thermal structure and aerosol distribution.*J. Geophys. Res.*, *106*, E10, 2156–2202. doi:10.1029/2000JE001321

[9] Warren, S.G., and Brandt, S.G., 2008. Optical constants of ice from the ultraviolet to the microwave: A revised compilation. *J. Geophys. Res.*, 113, D14220. doi:10.1029/2007JD009744

[10] Wolff, M.J., Smith, M.D., Clancy, R.T., Spanovich, N., Whitney, B.A., Lemmon, M.T., Bandfield, J.L., Banfield, D., Ghosh, A., Landis, G., Christensen, P.R., Bell III, J.F. and Squyres, S.W. (2006), Constraints on dust aerosols

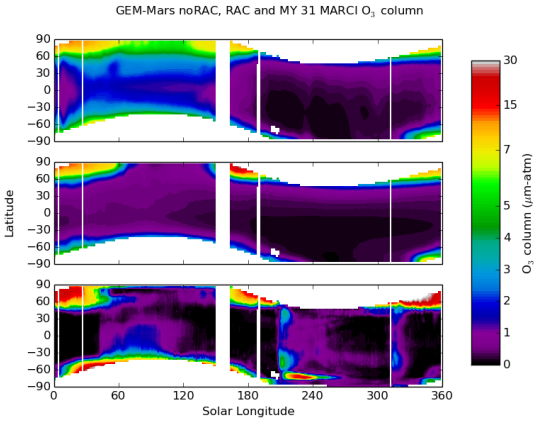

Figure 7: Column ozone compared with MARCI in μm-atm. Top: GEM-Mars noRAC, middle: GEM-Mars RAC, bottom: MARCI.

from the Mars Exploration Rovers using MGS overflights and Mini–TES, *J. Geophys.Res.*, *111*, E12S17. doi:10.1029/2006JE002786

[11] Wolff, M.J., Smith, M.D., Clancy, R.T., Arvidson, R., Kahre, M., Seelos, F., Murchie, S., and Savijärvi, H. 2009. Wavelength dependence of dust aerosol single scattering albedo as observed by the Compact Reconnaissance Imaging Spectrometer, *J. Geophys. Res.*, *114*, E00D04. doi:10.1029/2009JE003350